

Lane-changing in traffic streams

Jorge A. Laval^{*} and Carlos F. Daganzo[†]

April 8, 2005

Abstract. It is postulated that lane-changing vehicles create voids in traffic streams, and that these voids reduce flow. This mechanism is described with a model that tracks lane changers precisely, as particles endowed with realistic mechanical properties. The model has four easy-to-measure parameters and reproduces without re-calibration two bottleneck phenomena previously thought to be unrelated: *(i)* the drop in the discharge rate of freeway bottlenecks when congestion begins, and *(ii)* the relation between the speed of a moving bottleneck and its capacity.

^{*}Institute of Transportation Studies, University of California, Berkeley

[†]Department of Civil and Environmental Engineering, Transportation Group, University of California, Berkeley

1 Introduction

Freeway lane changing has received increased scientific attention during the last decade. Research has produced both qualitative conjectures [1–5] and empirical evidence [6–9], but a quantitative understanding of its impacts on traffic flow remains elusive.

This paper attempts to fill this gap. It considers freeway sections away from diverges, where the main incentive for drivers to change lanes is increasing their speed.¹ The main thesis is that a lane-changing vehicle acts as a moving bottleneck on its destination lane while accelerating to the speed prevailing on the lane, and that the ensuing disruption can trigger other lane changes. The freeway is therefore modeled as a set of interacting streams linked by the lane changes. The proposed model only needs one more parameter than the simplest traffic flow models (which require three) and explains several puzzling phenomena without re-calibration.

Existing traffic flow models do not address lane-changing phenomena properly. Extensions to kinematic wave (KW) theory [10, 11] with lane-changing [12–18] are inadequate because they treat lane-changing vehicles as a fluid that can accelerate instantaneously, and therefore do not sufficiently hinder following vehicles. Some microscopic simulation models consider realistic accelerations, but they have not yet been used successfully to model lane changes. Recent experience with these models [19] indicates that lane-changing greatly increases the complexity of the model specification and estimation process.

To overcome these problems, a hybrid approach was developed in [20]. It combines the best features of microscopic and macroscopic models: the parsimony of the KW model (for the traffic stream) with the accuracy of microscopic models (for slower vehicles). Slow vehicles are treated in this reference as moving bottlenecks in a single KW stream, as in the KW theory of moving bottlenecks [21–24]. Unfortunately, this requires as an input the maximum possible passing rates, which can only be guessed approximately.

This drawback is overcome in this paper by modeling each lane as a separate KW stream interrupted by lane-changing particles that completely block traffic; ie, that allow no passing on the lane they occupy. The incremental-transfer (IT) principle for multilane KW problems [15], coupled with a one-parameter model for lane-changing demand, is used to predict the flow transfers between neighboring lanes. The appendix describes the constrained-motion (CM) model of [20], which can capture a vehicle’s ability to accelerate after changing lanes recognizing both mechanical resistance and the restrictions imposed by downstream traffic. This CM model is used to generate particle trajectories. Section 2, below, describes the model and §3 evaluates it.

2 The model

The model is presented in two parts: §2.1 for the multilane KW module, and §2.2 for the lane-changing particles.

¹Generalizations to more complex geometries are easy to develop with the proposed modeling framework, but they require at least one more parameter to describe driver behavior. They will not be described here because they have not yet been tested.

47 2.1 The multilane KW module

A continuum multilane extension of the KW model for a highway with $n = 2$ lanes was first presented in [12]; see also [13, 14]. For $n > 2$ the conservation equation for a single lane, ℓ , is:

$$\frac{\partial k_\ell}{\partial t} + \frac{\partial q_\ell}{\partial x} = \Phi_\ell, \quad \ell = 1 \dots n, \quad (1)$$

48 where $k_\ell(t, x)$ and $q_\ell(t, x)$ give the density and flow on ℓ at the time-space point (t, x) . The
 49 inhomogeneous term Φ_ℓ is the *net lane-changing rate onto* lane ℓ , in units of veh/time-distance.
 50 It was postulated in [14] that Φ_ℓ was a linear function of the set of k_ℓ 's, but the idea was not
 51 applied successfully at the time because effective numerical methods [16, 25–27] had not yet
 52 been developed. The next two subsections show how the ideas in [12–14] can be refined and
 53 then implemented in discrete time.

54 2.1.1 The continuum formulation

Define the vector $k(t, x) \doteq [k_1(t, x), \dots, k_n(t, x)]$ and assume that the one-directional *lane-changing rate* from lane ℓ to lane ℓ' (with $\ell \neq \ell'$) is a function, $\Phi_{\ell\ell'}$, of k, t and x . The net lane-changing rates are related to the one-directional rates by:

$$\Phi_\ell = \sum_{\ell' \neq \ell} \Phi_{\ell'\ell} - \Phi_{\ell\ell'}. \quad (2)$$

The proposed model specifies the $\Phi_{\ell\ell'}$ instead of the Φ_ℓ and does not require linearity. The $\Phi_{\ell\ell'}$ must realistically represent the competition between drivers' desires for changing lanes, and the available space capacity in the target lane. To strike a balance between these two factors, we first specify three sets of functions of (k, t, x) defining: (i) a desired lane-changing rate from ℓ to ℓ' (ie, a demand for lane-changing in units of veh/time-distance) $L_{\ell\ell'}, \ell \neq \ell'$, (ii) a desired set of through flows on ℓ , T_ℓ , (in units of veh/time) and (iii) the available capacity on lane ℓ , μ_ℓ (in units of veh/time). Formally,

$$L_{\ell\ell'} = L_{\ell\ell'}(k, t, x), \quad (3a)$$

$$T_\ell = T_\ell(k, t, x), \quad (3b)$$

$$\mu_\ell = \mu_\ell(k_\ell, t, x). \quad (3c)$$

A competition mechanism, \mathcal{F} , then determines the actual one-directional lane-changing rates $\Phi_{\ell\ell'}$ and through flows q_ℓ from (3), ie

$$(\Phi_{\ell-1,\ell}, q_\ell, \Phi_{\ell+1,\ell}) \doteq \mathcal{F}(L_{\ell-1,\ell}, T_\ell, L_{\ell+1,\ell}, \mu_\ell). \quad (4)$$

55 Demand functions L and T are obtained by disaggregating with a choice model the sending
 56 (or demand) function of KW theory. The capacity function μ_ℓ is the receiving (or supply)
 57 function of KW theory [25, 26, 28]. The transformation \mathcal{F} should reflect sensible priority rules,
 58 which depend upon the nature of the lane-changing maneuvers (discretionary or mandatory).
 59 We will describe \mathcal{F} explicitly in the next section.

60 2.1.2 The discrete-time formulation

It is assumed here that the fundamental diagram (FD) of each lane is triangular with free-flow speed u , wave speed $-w$ and jam density κ . (This accounts for three of the four model parameters.) All lanes are partitioned into small cells of length Δx and time is discretized into steps of duration Δt ; see Fig. 1. The following three-dimensional grid is used: $(t_j \doteq j\Delta t, x_i \doteq i\Delta x, \ell)$. For numerical stability it is assumed that:

$$\Delta x \doteq u\Delta t. \quad (5)$$

Indices i and j will be used to denote the calculated values of a variable at a discrete point (t_j, x_i) ; eg, $k_{i\ell}^j$ will denote the discrete approximation of $k_\ell(t_j, x_i)$. In the discrete world, the conservation equation becomes

$$\frac{k_{i\ell}^{j+1} - k_{i\ell}^j}{\Delta t} + \frac{q_{i\ell}^j - q_{i-1,\ell}^j}{\Delta x} = \sum_{\ell' \neq \ell} \Phi_{i-1,\ell'\ell}^j - \Phi_{i\ell\ell'}^j, \quad \forall \ell. \quad (6)$$

61 This equation is ready for stepping through time, since there is only one term with time index
 62 $j + 1$. At each iteration one calculates $L_{i\ell\ell'}^j, T_{i\ell}^j$ and $\mu_{i\ell}^j$ for every cell (i, ℓ) with (3) using the
 63 current densisites k^j as arguments. One then computes the lane-changing rates and through
 64 flows $q_{i\ell}^j, q_{i-1,\ell}^j, \Phi_{i-1,\ell'\ell}^j$ and $\Phi_{i\ell\ell'}^j$ with the IT principle (4) and then evaluates $k_{i\ell}^{j+1}$ with (6). We
 65 now explain how to compute these rates with the IT principle.

66 Recipes for L, T and μ

As a first step we specify the arguments of the IT recipe: $L_{i\ell\ell'}^j, T_{i\ell}^j$ and $\mu_{i\ell}^j$. Recall that the sending function for triangular FDs gives the desired aggregate number of advancing moves in Δt ; ie

$$S_{i\ell}^j \doteq \Delta t \min\{uk_{i\ell}^j, Q\}. \quad (7)$$

Recipe for L : The desired number of lane-changing moves in Δt is given by

$$L_{i\ell\ell'}^j \Delta t \Delta x \doteq \pi_{i\ell\ell'}^j \Delta t S_{i\ell}^j, \quad \forall \ell, \forall \ell' \neq \ell, \quad (8)$$

where $\pi_{i\ell\ell'}^j$ is the fraction of choice-makers per unit time wishing to change from lane ℓ to lane ℓ' . We assume for maximum simplicity that the choice probability rate $\pi_{i\ell\ell'}^j$ is proportional to the positive speed difference between lanes, $\Delta v_{i\ell\ell'}^j \doteq \max\{0, v_{i\ell'}^j - v_{i\ell}^j\}$, where $v_{i\ell}^j$ is the average speed on lane ℓ ; ie²

$$\pi_{i\ell\ell'}^j \doteq \frac{\Delta v_{i\ell\ell'}^j}{u\tau}, \quad \forall \ell, \forall \ell' \neq \ell, \quad (9)$$

67 where the parameter τ has units of time. Notice that τ^{-1} is an upper bound to $\pi_{i\ell\ell'}^j$; as such,
 68 τ can be interpreted as the time a driver takes to decide and execute a lane change when the
 69 origin lane is stopped and the target lane is freely-flowing.

²We propose using Eddie's generalized space-mean speed on a look-ahead section downstream of the current position during an evaluation period immediately preceding the current instant. Our tests used negligible evaluation periods and a look-ahead section comparable with the vehicle spacing.

Recipe for T : It follows from the definition of $\pi_{i\ell\ell'}^j$ that the probability of staying in the same lane in the next Δt is $1 - \sum_{\ell' \neq \ell} \pi_{i\ell\ell'}^j \Delta t$, which will be in $(0, 1]$ if we choose $\Delta t \ll \tau$. Thus, the desired number of through moves in the next Δt is

$$T_{i\ell}^j \Delta t \doteq (1 - \sum_{\ell' \neq \ell} \pi_{i\ell\ell'}^j \Delta t) S_{i\ell}^j, \quad \forall \ell. \quad (10)$$

Recipe for μ : The available capacity is given by the receiving function for a triangular FD:

$$\mu_{i\ell}^j \Delta t \doteq \Delta t \min\{w(\kappa - k_{i\ell}^j), Q\}, \quad \forall \ell. \quad (11)$$

70 IT principle

We now show how the IT principle transforms the values of $L_{i\ell\ell'}^j$, $T_{i\ell}^j$ and $\mu_{i\ell}^j$ for every cell into the actual lane-changing rates and through flows. The IT recipe allocates differentials of flow to the desired target cell (i, ℓ) on a first-come-first-served basis. (We now drop the subindexes i and j for clarity). When total demand $T_\ell + \sum_{\ell' \neq \ell} \Delta x L_{\ell'\ell}$ is less than the available capacity μ_ℓ all the demands are fulfilled and able to advance to the target cell; otherwise the IT recipe prorates that available capacity to the different origin lanes according to their demands. It has been shown in [29] that if γ_ℓ represents the fraction of the demand able to advance the IT result reduces to

$$\gamma_\ell \doteq \min\left\{1, \frac{\mu_\ell}{T_\ell + \sum_{\ell' \neq \ell} \Delta x L_{\ell'\ell}}\right\}, \quad (12)$$

and the transfers to the target lane ℓ are

$$\Phi_{\ell'\ell} = \gamma_\ell L_{\ell'\ell}, \quad \forall \ell' \neq \ell, \quad (13a)$$

$$q_\ell = \gamma_\ell T_\ell. \quad (13b)$$

71 Similar formulae have been proposed in [30] for intersection modeling.

The quantities in (13) can be understood physically by taking the limit $\Delta t, \Delta x \rightarrow 0$. For example, consider a steady-state case where total demand exceeds available capacity. Combining (13) and (12) we find

$$\Phi_{\ell'\ell} = \frac{\mu_\ell}{T_\ell + \sum_{\ell' \neq \ell} \Delta x L_{\ell'\ell}} L_{\ell'\ell}. \quad (14)$$

Using (8) and (10) in (14) and after manipulation one obtains

$$\lim_{\Delta x \rightarrow 0} \Phi_{\ell'\ell} = \frac{\mu_\ell \pi_{\ell'\ell} S_{\ell'}}{u S_\ell}. \quad (15)$$

72 This shows that the $\Phi_{\ell'\ell}$'s tend to finite values as the mesh size tends to zero. Similarly, it
 73 can be shown that $q_\ell \rightarrow \mu_\ell$. In fact, manipulation of (5)-(13) reveals that the discrete model
 74 expresses a relationship between meaningful physical variables in the limit of $\Delta t, \Delta x \rightarrow 0$.
 75 Thus, Δt and Δx are not parameters of the model; they should be simply chosen as small as

76 possible. This is reasonable; it was shown in [31] that model (5)-(13) is numerically stable and
77 converges to a continuum solution in the dynamic case as the lattice is refined.

78 This completes the formulation of the discrete algorithm. More details can be found in
79 [32]. Note that equations (5)-(13) have only introduced one additional parameter, τ . The
80 model, however, is not yet sufficiently realistic. As its predecessors [12–14], it ignores that the
81 disruption caused by a lane change depends on the initial speed of the lane-changing vehicle
82 and on its ability to accelerate. As a result, it underestimates the disruption caused by the lane
83 changes. The following subsection shows how to remedy this problem.

84 **2.2 Discrete lane-changing particles**

85 The basic idea consists in quantizing the lane-changing rates from model (5)-(13) to generate
86 discrete particles, and then treating them with the method in [33] as temporary blockages
87 that move with bounded accelerations. This is possible because the blockages have a known
88 (zero) passing rate and trajectories that can be determined endogenously with the CM model
89 of vehicle dynamics. In the CM model, particles move with maximum acceleration, but are
90 constrained by their own power and the speed of traffic ahead [20]. A distinguishing feature
91 of the method is that particles are tracked with very high resolution in continuous space (no
92 jumping).

93 To quantize the process we can simply evaluate the cumulative number of lane changes from
94 (i, ℓ) to $(i + 1, \ell')$ by time t_j , $\eta_{i\ell\ell'}^j \doteq \sum_{j' \leq j} \Phi_{i\ell\ell'}^{j'} \Delta t \Delta x$, and then use the “floor” function $\lfloor \eta_{i\ell\ell'}^j \rfloor$
95 to generate integer jumps. In our tests, we added a degree of randomness of people’s choices,
96 by generating particles as outcomes of Poisson variables with mean $\eta_{i\ell\ell'}^j - \eta_{i\ell\ell'}^{j-1}$, but this did
97 not change the macroscopic results.

98 The complete hybrid model has good estimation and convergence properties. It is parsimo-
99 nious since it only requires the relaxation time for lane-changing, τ , and the three usual KW
100 parameters (free-flow speed, capacity and jam density), which are readily observed in the field.
101 It continues to converge as $\Delta t \rightarrow 0$, since the introduction of discrete moving bottlenecks is
102 akin to the specification of additional boundary conditions, as explained in [27].

103 **3 Empirical tests and discussion**

104 All the numerical experiments assume that $\tau = 3$ secs and the triangular FD on each lane has
105 free-flow speed $u = 96.6$ km/h (60 mph), congested wave speed $w = -24$ km/h (-15 mph) and
106 jam density per lane $\kappa = 93.2$ vpkpl (150 vpmpl). Additionally, all lane-changing vehicles are
107 assumed to have the acceleration capabilities of a typical car. We used $\Delta t = 0.3$ sec, but the
108 results are insensitive to values in (0, 0.5) sec.

109 **3.1 Lane-drops**

110 Recent experiments [34] show a consistent reduction in discharge flow after the onset of con-
111 gestion at bottlenecks caused by lane-drops. A similar reduction has been observed at merge
112 bottlenecks [9]. This suggests that the drop in discharge rate may be caused by lane changers –
113 since approaching mainline vehicles are forced away from the shoulder lane in both bottleneck
114 configurations. We now explore this conjecture.

115 The proposed model was applied to a 0.5 km (0.31 mi) 3-lane freeway with a lane-drop at
 116 $x = 0.33$ km (0.2 mi); see Fig. 2. At $t = 0$ the freeway is empty and the input demand is held
 117 constant at 1,242 vph on the median and middle lanes (lanes 1 and 2, respectively) and 416 vph
 118 on the shoulder lane (lane 3). The cumulative count curves across all lanes, $N(t)$, produced by
 119 the proposed method for the four locations shown in Fig. 2 are shown in Fig. 3a. Curves are
 120 plotted on an oblique coordinate system with a “background flow” of 2630 vph. They show
 121 that flow drops from 2900 vph to 2630 vph around $t = 10$ min. This is a 9.3% drop. The
 122 magnitude of the drop varies across simulations and demand patterns but only slightly. The
 123 results are consistent with [34].

124 Parts (b) and (c) of Fig. 3 show that the results of the simulation are also in agreement with
 125 the findings of ongoing finer-resolution empirical studies at merge bottlenecks [8]. These studies
 126 show that the reduction in bottleneck discharge rate occurs simultaneously with sharp increases
 127 in both, vehicular accumulation and lane-changing activity upstream of the bottleneck. Part
 128 (b) of the figure shows the lane-specific vehicle accumulation predicted by the model for 0.23
 129 $\text{km} \leq x \leq 0.33$ km; notice how the increase in accumulation (on all lanes) correlates nearly
 130 perfectly with the flow drop of part (a). Part (c) shows the cumulative number of lane changes
 131 upstream of the bottleneck on an oblique coordinate system with a background rate of 337 lane
 132 changes per hour. Notice how in this case too the lane-changing rate increases significantly
 133 in conjunction with the breakdown. Note too that the increase is roughly linear and that it
 134 stabilizes at a level of about 600 lane changes per hour. Reference [8] also found a linearly
 135 increasing rate and similar stabilization level.

136 All in all, the evidence strongly suggests that lane changes are the main cause of the drop
 137 in discharge rate, and that the proposed model can roughly capture the effect.

138 3.2 Moving obstructions

Reference [24] describes the results of several experiments where obstructions with a range of
 controlled speeds v were introduced in two freeways. It was found that there was a reproducible
 relation between the capacity of the moving bottleneck, Q_m (the queue discharge rate,) and v ,
 ie

$$Q_m = Q_m(v), \quad \text{with } \frac{dQ_m}{dv} > 0 \text{ for } v > 50 \text{ km/h.} \quad (16)$$

139 This phenomenon is still not well understood. Existing theories either assume that $\frac{dQ_m}{dv} = 0$
 140 (see [22, 23, 35]), or introduce (16) as an exogenous boundary condition [20]. By doing this,
 141 however, all the factors that could affect capacity are ignored.

142 To test the proposed theory we simulated the experiments in [24] for a broader set of
 143 conditions: $v \in \{0, \dots, 80\}$ km/h and $n \in \{2, 3, 4\}$. Figure 4 plots the results. It displays the
 144 (normalized) capacity, $\rho = Q_m(v)/Q_m(u)$, versus v . The match with empirical data (circles in
 145 the figure) is reasonably good, considering that no parameters were re-calibrated.

146 Curiously, the model predicts two regimes. Regime 1 ($v > 20$ km/h) where $\rho(v)$ increases,
 147 and regime 2 ($v < 20$ km/h) where $\rho(v)$ slightly decreases. Although [24] does not include
 148 experiments in regime 2, we note from §3.1 that the hybrid model predicts $\rho(0)$ reasonably
 149 well. Thus, the slight trend reversal is probably real.

150 The two-regime phenomenon is qualitatively explained by the spatial distribution of the
 151 lane changes. Figure 5 shows the k -maps for one simulation for two bottleneck speeds, $v = 1$

152 and 32 km/h. Lane-changing locations are depicted as bold dots. Note from the white regions
153 how lane changes reduce the flow downstream of the moving obstruction, as expected. The key
154 observation here is that the closer a maneuver is to the bottleneck the bigger the void in front of
155 the lane-changer. This is because lane-speed differences are greater close to the bottleneck. The
156 reason for the capacity trend in regime 1 (Fig. 5b) is a direct consequence of this effect, because
157 as v increases lane-speed differences drop and lane-changing becomes less and less disruptive.

158 Note now from Fig. 5a (regime 2) that there is a critical distance from the bottleneck beyond
159 which lane-changing has no effect. Furthermore, for very low speeds a significant number of
160 lane changes occur beyond this critical distance. The trend of regime 2 is then explained,
161 because as $v \rightarrow 0$ more and more lane changes take place far upstream from the bottleneck
162 where lane-speeds are similar. We recognize that these results could vary slightly with a more
163 realistic lane-choice model, but they clearly illustrate the deleterious effect of lane changes near
164 a bottleneck.³

165 3.3 Discussion

166 A four-parameter multilane hybrid model for traffic flow that recognizes the bounded accelera-
167 tions of lane-changing vehicles has been introduced. The model appears to explain the reduction
168 in flow observed after the onset of congestion at freeway lane-drops and the relationship between
169 the speed of moving bottlenecks and their capacities. The ultimate cause for both phenomena
170 appears to be the limited ability of lane changers to accelerate. (Additional simulations show
171 that both effects disappear when the acceleration parameter of the model is increased.) The
172 more detailed evidence also suggests that lane changes affect bottleneck behavior in ways that
173 can be controlled to improve traffic flow. For example, since the spatial distribution of lane
174 changes and the difference in lane speeds are found to be important determinants of bottleneck
175 capacity, traffic managers may be able to increase capacity by forbidding lane changes and/or
176 posting speed advisories at key locations upstream of bottlenecks; eg, as in [36].

177 We obtained virtually identical results after replacing the KW module with the cellular
178 automata (CA) model in [37], using the same three macroscopic parameters. (This reference
179 shows that the vehicle trajectories produced by the CA model in that reference and the KW
180 model with triangular FD produce the same vehicle trajectories to within a tolerance of a sin-
181 gle jam spacing.) Thus, the predictions of the theory appear to be insensitive to the type of
182 approximation (continuum/discrete) used for the traffic streams. Preliminary research also re-
183 veals that the model reproduces other phenomena quite well: the slow growth of instabilities in
184 queued traffic, the emergence of synchronized FIFO traffic in space-time, and the lane-changing
185 rates observed at merge bottlenecks during the “drop to capacity”. This universality suggests
186 that the proposed lane-changing theory should be also helpful in settings that require com-
187 plex vehicle maneuvers, such as freeways with diverges and weaves, and surface streets with
188 signalized intersections. The necessary extensions are easy to implement because any type of
189 maneuver can be handled naturally within the proposed framework. The theory should of
190 course be tested in complex environments once reliable data become available.

191

³A more realistic lane-choice model would recognize drivers’ reluctance to change lanes with very high speed differences.

192 *Acknowledgment- This research was partially funded by the International Center of Excel-*
193 *lence on Future Urban Transport at the University of California, Berkeley, and by the University*
194 *of California Transportation Center.*

References

- 196 [1] M Brackstone, M McDonald, and J Wu. Lane changing on the motorway : factors affecting
 197 its occurrence, and their implications. In *9th International Conference on Road Transport*
 198 *Information and Control*, London, UK, 1998.
- 199 [2] GL Chang and YM Kao. An empirical investigation of macroscopic lane-changing char-
 200 acteristics on uncongested multilane freeways. *Transportation Research A*, 25(6):375–389,
 201 1991.
- 202 [3] D Chowdhury, DE Wolf, and M Schreckenberg. Particle hopping models for two-lane traffic
 203 with two kinds of vehicles: Effects of lane-changing rules. *Physica A*, 235(3-4):417–439,
 204 1997.
- 205 [4] CH Wei, E Meyer, J Lee, and C Feng. Characterizing and modeling observed lane-changing
 206 behavior: lane-vehicle-based microscopic simulation on urban street network. *Transporta-*
 207 *tion Research Records, TRB*, (1710):104–113, 2000.
- 208 [5] JM Greenberg, A Klar, and M Rasche. Congestion on multilane highways. *SIAM journal*
 209 *of applied mathematics.*, 63(3):813–818, 2003.
- 210 [6] M Mauch and MJ Cassidy. Freeway traffic oscillations: Observations and predictions. In
 211 M.A.P. Taylor, editor, *15th Int. Symp. on Transportation and Traffic Theory*, Pergamon-
 212 Elsevier, Oxford,U.K., 2002.
- 213 [7] S Ahn. *Growth of oscillations in queued traffic*. PhD thesis, Dept. of Civil Engineering,
 214 Univ. of California, Berkeley, 2005.
- 215 [8] M Cassidy and J Rudjanakanoknad. Increasing capacity of an isolated merge by metering
 216 its on-ramp. *Trans. Res. B, In Press*, 2005.
- 217 [9] M Cassidy and R Bertini. Some traffic features at freeway bottlenecks. *Trans. Res. B*, 1
 218 (33):25–42, 1999.
- 219 [10] MJ Lighthill and GB Whitham. On kinematic waves. I Flow movement in long rivers. II
 220 A theory of traffic flow on long crowded roads. *Proc. Roy. Soc.*, 229(A):281–345, 1955.
- 221 [11] P I Richards. Shockwaves on the highway. *Opns. Res.*, (4):42–51, 1956.
- 222 [12] PK Munjal and LA Pipes. Propagation of on-ramp density perturbations on unidirectional
 223 two- and three-lane freeways. *Transportation Research B*, 5(4):241–255, 1971.
- 224 [13] PK Munjal, Y Hsu, and RL Lawrence. Analysis and validation of lane-drop effects on
 225 multi-lane freeways. *Transportation Research B*, 5(4):257–266, 1971.
- 226 [14] PG Michalopoulos, DE Beskos, and Y Yamauchi. Multilane traffic dynamics: Some macro-
 227 scopic considerations. *Trans. Res. B*, (18):377–395, 1984.
- 228 [15] C F Daganzo. A continuum theory of traffic dynamics for freeways with special lanes.
 229 *Trans. Res. B*, 2(31):83–102, 1997.

- 230 [16] CF Daganzo, W Lin, and J Del Castillo. A simple physical principle for the simulation of
231 freeways with special lanes and priority vehicles. *Trans. Res. B*, 2(31):105–125, 1997.
- 232 [17] C F Daganzo. A behavioral theory of multi-lane traffic flow part I: Long homogeneous
233 freeway sections. *Trans. Res. B*, 2(36):131–158, 2002.
- 234 [18] C F Daganzo. A behavioral theory of multi-lane traffic flow part II, merges and the onset
235 of congestion. *Trans. Res. B*, 2(36):159–169, 2002.
- 236 [19] C Buisson and P Wagner. Calibration and validation of simulation models: A tutorial.
237 Presented at TRB 2004 annual meeting. Workshop 148: Traffic simulation models. Wash-
238 ington, USA, 2004.
- 239 [20] JA Laval and CF Daganzo. A hybrid model of traffic flow: Impacts of roadway geometry
240 on capacity. *TRB 2003 Annual Meeting CD-ROM. Submitted for publication.*, 2003.
- 241 [21] G F Newell. A moving bottleneck. Technical Report UCB-ITS-RR-93-3, Inst. Trans.
242 Studies, Univ. of California, Berkeley, CA, 1993.
- 243 [22] G F Newell. A moving bottleneck. *Trans. Res. B*, (32):531–537, 1998.
- 244 [23] JP Lebacque, JB Lesort, and F Giorgi. Introducing buses into first-order macroscopic
245 traffic flow models. *Trans. Res. Rec.*, (1644):70–79, 1998.
- 246 [24] JC Muñoz and CF Daganzo. Moving bottlenecks: a theory grounded on experimental
247 observation. In M.A.P. Taylor, editor, *15th Int. Symp. on Transportation and Traffic
248 Theory*, pages 441–462, Pergamon-Elsevier, Oxford,U.K., 2002.
- 249 [25] C F Daganzo. The cell-transmission model: A dynamic representation of highway traf-
250 fic consistent with the hydrodynamic theory. Technical Report UCB-ITS-RR-93-7, Inst.
251 Trans. Studies, Univ. of California, Berkeley, CA, 1993.
- 252 [26] J P Lebacque. The godunov scheme and what it means for first order traffic flow models. In
253 J. B. Lesort, editor, *13th Int. Symp. on Transportation and Traffic Theory*, pages 647–678,
254 Elsevier, New York, 1996.
- 255 [27] C F Daganzo. A variational formulation of kinematic wave theory: basic theory and
256 complex boundary conditions. *Trans. Res. B*, 2(39):187–196, 2003.
- 257 [28] C F Daganzo. The cell transmission model: A dynamic representation of highway traffic
258 consistent with the hydrodynamic theory. *Trans. Res. B*, 4(28):269–287, 1994.
- 259 [29] L Leclercq. Private communication. 2004.
- 260 [30] JP Lebacque and JB Lesort. Macroscopic traffic flow models: a question of order. In
261 A. Ceder, editor, *14th Int. Symp. on Transportation and Traffic Theory*, pages 3–25, Perg-
262 amon, New York, N.Y., 1999.
- 263 [31] J A Laval. Some properties of a multi-lane extension of the kinematic wave model. *TRB
264 2003 Annual Meeting CD-ROM. Also ITS Tech. Report UCB-ITS-WP-2003-1*, 2003.

- 265 [32] J A Laval. *Hybrid models of traffic flow: impacts of bounded vehicle accelerations*. PhD
266 thesis, Dept. of Civil Engineering, Univ. of California, Berkeley, 2004.
- 267 [33] CF Daganzo and JA Laval. Moving bottlenecks: A numerical method that converges in
268 flows. *Trans. Res. B*, 9(39):855–863, 2005.
- 269 [34] RL Bertini and MT Leal. Empirical study of traffic features at a freeway lane drop. *Trans.*
270 *Res. A (Submitted)*, 2004.
- 271 [35] F Giorgi, L Leclercq, and JB Lesort. A traffic flow model for urban traffic analysis:
272 extensions of the LWR model for urban and environmental applications. In M.A.P. Taylor,
273 editor, *15th Int. Symp. on Transportation and Traffic Theory*, pages 393–415, Pergamon-
274 Elsevier, Oxford,U.K., 2002.
- 275 [36] CF Daganzo, JA Laval, and JC Muñoz. Some ideas for freeway congestion mitigation with
276 advanced technologies. *Traffic Engineering and control*, 10(43):397–403, 2002.
- 277 [37] C F Daganzo. In traffic flow, cellular automata = kinematic waves. Technical Report
278 UCB-ITS-RR-2004-5, Inst. Trans. Studies, Univ. of California, Berkeley, CA, 2004.
- 279 [38] CF Daganzo and JA Laval. On the numerical treatment of moving bottlenecks. *Trans.*
280 *Res. B*, 1(39):31–46, 2005.
- 281 [39] A Gazizadeh, A Fahim, and M El-Gindy. Neural network representation of a vehicle
282 dynamics: Neuro-vehicle. *Int Journal of Vehicle Design*, 17(1), 1996.
- 283 [40] M W Sayers and S M Riley. Modeling assumptions for realistic multibody simulations of
284 the yaw and roll behavior of heavy trucks. In *SAE, International Congress and Exposition*.
285 Detroit, USA, 1996.
- 286 [41] X Tong, B Tabarrok, and M El-Gindy. Dynamics of logging trucks. *Heavy Vehicle Systems,*
287 *special series, of Int. J. of Vehicle Design*, 5(1), 1998.
- 288 [42] TD Gillespie and MW Sayers. A multibody approach with graphical user interface for sim-
289 ulating truck dynamics. Technical report, Michigan University, Ann Arbor, Transportation
290 Research Institute, Great Lakes Center for Truck and Transit Research, 1999.
- 291 [43] FHWA. The capability and enhancement of VDANL and TWOPAS for analyzing vehic-
292 ular performance on upgrades and downgrades within IHSDM. Technical Report 00-078,
293 Federal Highway Administration, 2000.
- 294 [44] Z Jiang, DA Streit, and M El-Gindy. Heavy vehicle ride comfort: Literature survey. *Heavy*
295 *Vehicle Systems, special series, of Int. J. of Vehicle Design*, 8(3):258–284, 2001.
- 296 [45] H Rakha, I Lucic, S Demarchi, J Setti, and M Van Aerde. Vehicle dynamics model for
297 predicting maximum truck acceleration levels. *Journal of transportation engineering*, pages
298 418–425, 2001.

299 **List of Figures**

300 1 Discretized freeway representation. 14
301 2 Simulation of a lane-drop: configuration and snapshot at $t = 11$ min. 15
302 3 Simulation of a lane-drop:(a) rescaled N -curves produced by the model; (b)
303 vehicle accumulation on all lanes for $0.23 \text{ km} \leq x \leq 0.33 \text{ km}$; (c) cumulative
304 number of lane changes upstream of the bottleneck. 16
305 4 Dimensionless bottleneck discharge rate, ρ , as a function of the slow vehicle speed
306 v for $n \in \{2, 3, 4\}$ lanes. 17
307 5 k -maps for a moving obstruction traveling at (a) $v = 1$ kph and (b) $v = 50$ kph. . 17

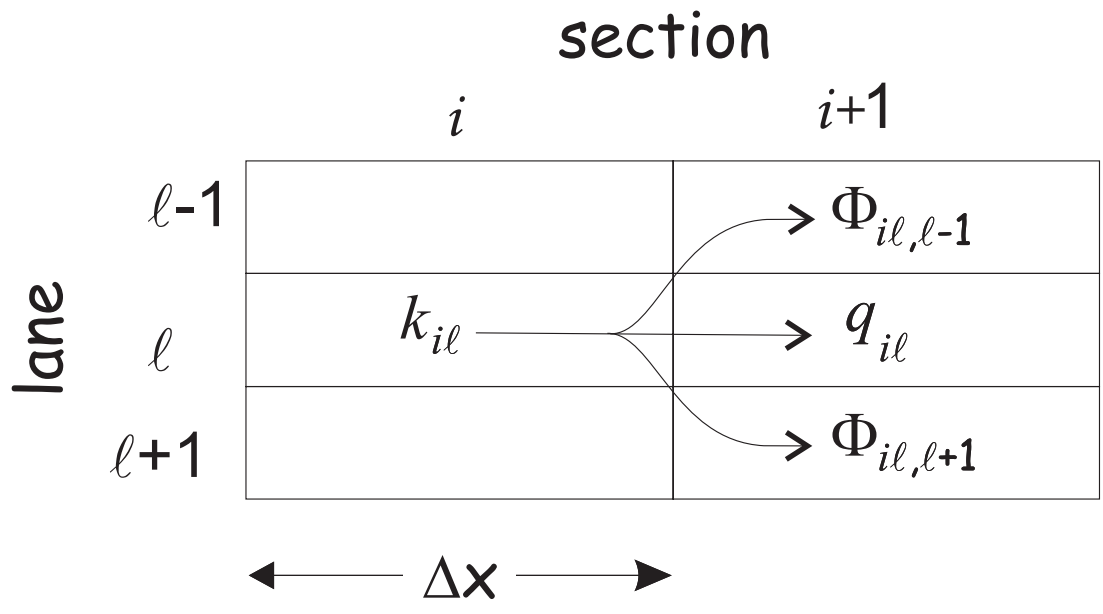


Figure 1: Discretized freeway representation.

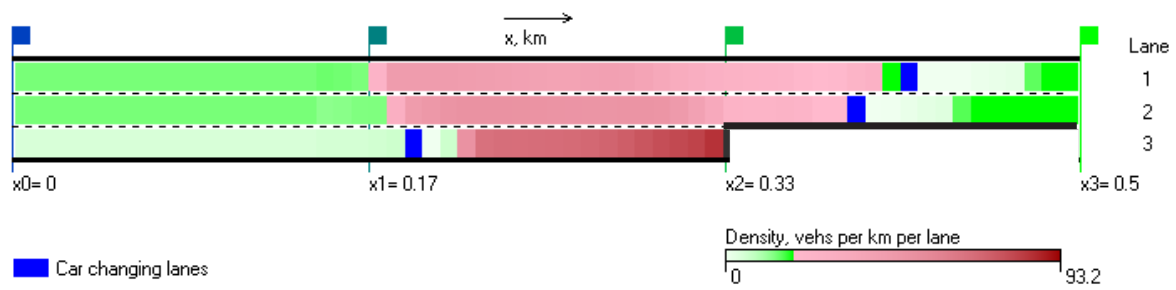


Figure 2: Simulation of a lane-drop: configuration and snapshot at $t = 11$ min.

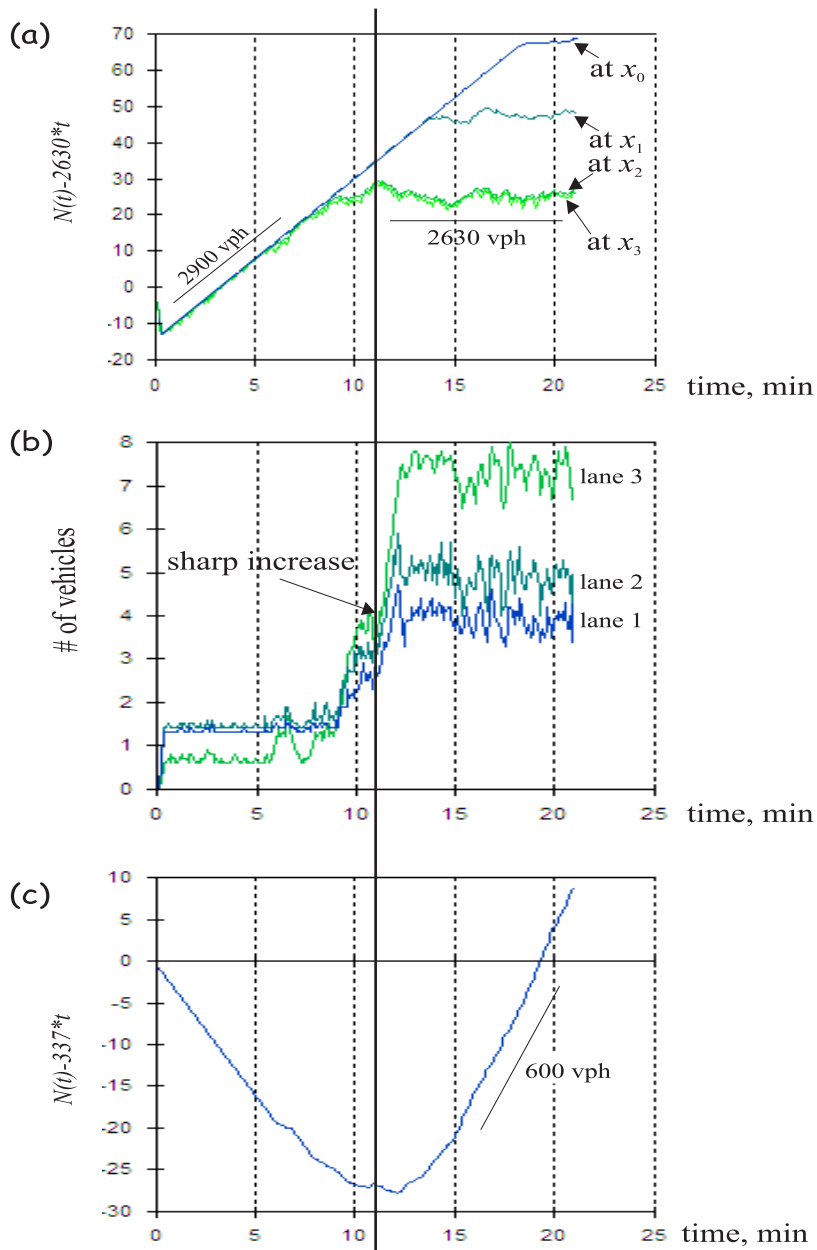


Figure 3: Simulation of a lane-drop:(a) rescaled N -curves produced by the model; (b) vehicle accumulation on all lanes for $0.23 \text{ km} \leq x \leq 0.33 \text{ km}$; (c) cumulative number of lane changes upstream of the bottleneck.

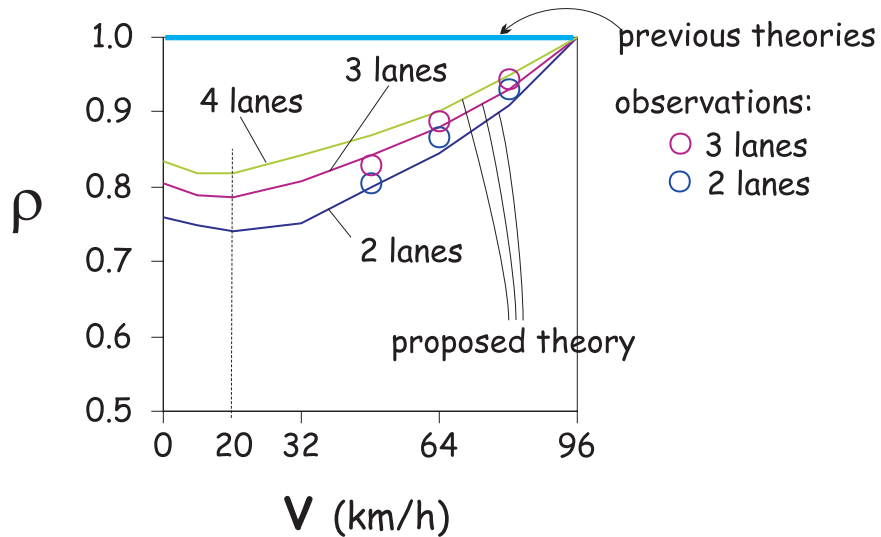


Figure 4: Dimensionless bottleneck discharge rate, ρ , as a function of the slow vehicle speed v for $n \in \{2, 3, 4\}$ lanes.

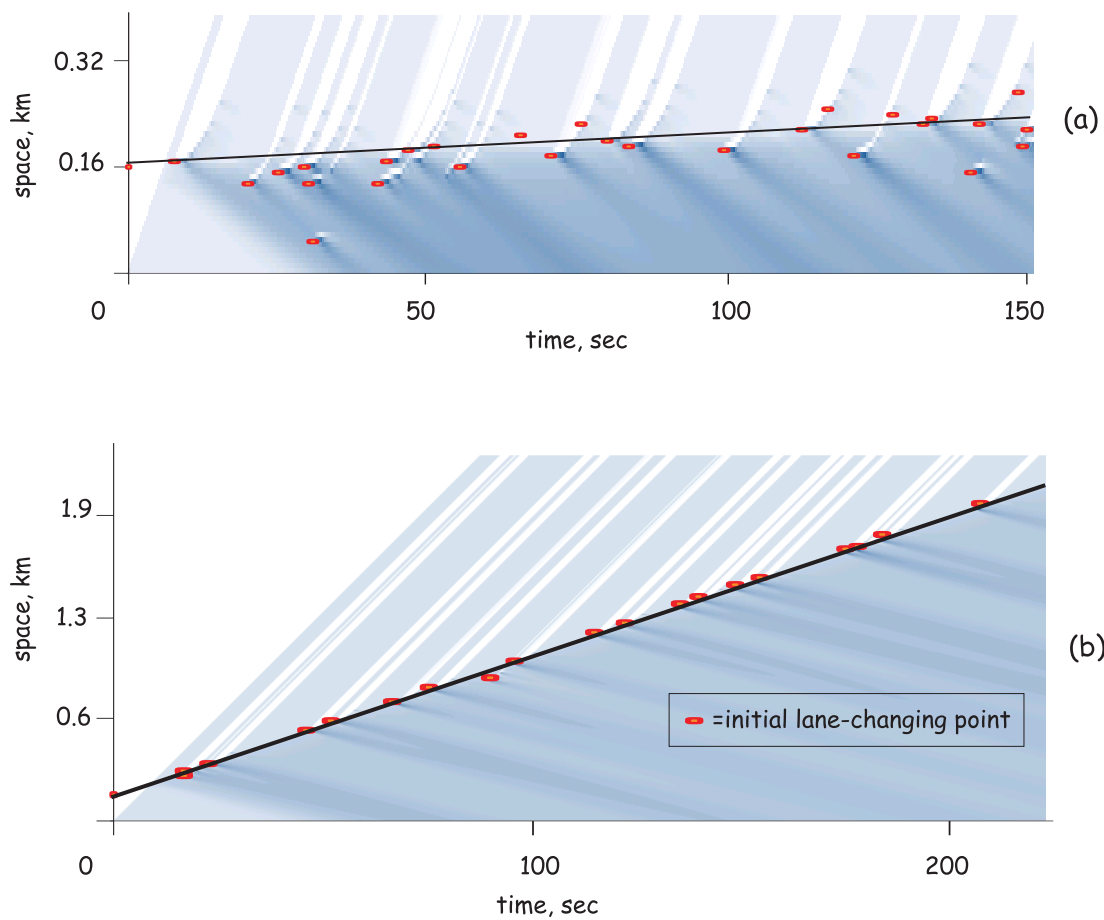


Figure 5: k -maps for a moving obstruction traveling at (a) $v = 1$ kph and (b) $v = 50$ kph.

A The Constrained Motion model

Let $x = \phi(t)$ be the position, x , of a moving bottleneck (MB) at time t . Its desired acceleration $a(v(t), x)$ is given by (A4) in the next subsection. We use the following constrained motion rule for vehicles kinetics, were the MB's current speed, $v(t)$, is constrained both by its ability to accelerate and by traffic downstream, ie

$$v(t) = \min\{v_{\text{down}}(t), v_{\text{des}}(t)\}, \quad (\text{A1})$$

where $v_{\text{down}}(t)$ is a numerical estimate in $[t, t + \Delta t)$ for the speed of the KW stream immediately downstream of the MB, and on the lane occupied by the MB. Notice that $v_{\text{down}}(t)$ cannot exceed u . The $v_{\text{des}}(t)$ is the ‘‘desired’’ MB speed, obtained with the relation

$$v_{\text{des}}(t + \Delta t) \doteq v(t) + a(v(t), \phi(t))\Delta t. \quad (\text{A2})$$

The MB's position is then updated with

$$\phi(t + \Delta t) = \phi(t) + v(t)\Delta t. \quad (\text{A3})$$

309 To estimate the effects of the MB on the rest of the traffic stream and calculate $v_{\text{down}}(t)$, we
 310 use the method in Daganzo and Laval [38]. The overall procedure is made up of numerically
 311 stable components. As expected, it tends to the continuum solution as $\Delta t \rightarrow 0$ in all the
 312 numerical experiments in [20].

313 A.1 Free motion models

314 Free-motion models for the kinematics of an isolated vehicle [39–45] capture the physical lim-
 315 itations imposed by roadway geometry on the engine for typical driver behavior. Based on
 316 Newtonian mechanics, they give the ‘‘desired’’ acceleration of a vehicle, $a(\cdot)$, as a function of
 317 its current speed $v(t)$, and the vehicle and road characteristics.

The free-motion model for cars incorporated in TWOPAS [43] is used in this paper. It takes a linear form that depends on the grade at location x expressed as a decimal, $G(x)$, and on the car's maximum speed, v_{max} , and zero-speed acceleration, a_0 :

$$a = a_0(1 - v/v_{\text{max}}) - gG. \quad (\text{A4})$$

318 where $g = 9.81 \text{ m/s}^2$ is the acceleration of gravity. The car type used in the numerical demon-
 319 strations of §3 is a high performance car, defined with $v_{\text{max}} = 155 \text{ km/h}$ and $a_0 = 4.3 \text{ m/s}^2$.